

Final report on the project entitled “Collective properties of dislocations”

The main objective of the work proposed in the project was the experimental and theoretical investigation of the statistical properties of the deformation of micron sized objects. The research carried out can be separated into five different tasks.

Developing a continuum theory of dislocations

According to recent experimental and numerical investigations if a characteristic length (like grain size) of a specimen is in the submicron size regime several new interesting phenomena emerge during the deformation. Since in such systems boundaries play a crucial role, to model the plastic response it is crucial to determine the dislocation distribution near the boundaries. We proposed a phase field type continuum theory of the time evolution of an ensemble of parallel edge dislocations with identical Burgers vectors, corresponding to the dislocation geometry near internal boundaries. In order to account for the strong variation of the dislocation density (denoted by ρ_+) near the boundaries observed by discrete dislocation dynamics (DDD) simulation (see Fig. 1) we had to introduce gradient

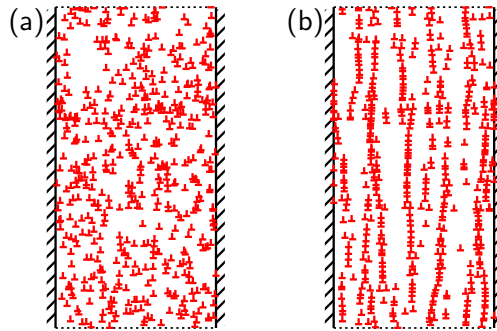


Figure 1: (a) Random initial configuration of dislocations in a channel. (b) Relaxed dislocation configuration. The boundaries in x direction are impenetrable and periodic boundary condition is used in the y direction. It is mentioned, that the channel is embedded in a medium infinite in the x direction.

like and surface terms into the phase field dislocation continuum theory we proposed earlier. The phase field functional suggested reads as:

$$P(\rho_+, \chi) = \int_D \left\{ -\frac{D}{2} (\Delta \chi)^2 + b \chi \partial_y \rho_+ + T \rho_+ \left[\ln \left(\frac{\rho_+}{\rho_0} \right) + u_0 \left(\frac{\nabla \rho_+ \hat{S} \nabla \rho_+}{2 \rho_+^3} \right) \right] \right\} dx dy + \oint_{\partial D} \alpha_{sf} T \sqrt{\rho_+} \vec{n} d\vec{A}$$

where χ is the stress potential generated by the dislocation system, D , T , ρ_0 , u_0 , and α_{sf} are constants, and \hat{S} is a 2x2 constant matrix. According to the standard formalism of phase field theory for conserved quantities the evolution equation of the dislocation density reads as

$$\dot{\rho}_+ + \partial_x j_+ = 0 \quad \text{with} \quad j_+ = M \left[\rho_+ \partial_x \frac{\delta P}{\delta \rho_+} \right].$$

An important nonstandard feature of the above evolution equation is that $M[x]$ is a nontrivial on/off type mobility function preventing the evolution of the dislocation density if the internal stress related to dislocation-dislocation correlations is smaller than a critical value (for details see [4]). A direct

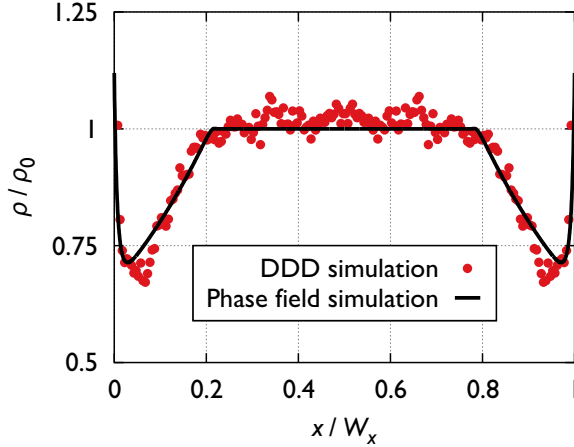


Figure 2: Dislocation density profiles (relative to the initial density), averaged in the direction perpendicular to the slip direction, developing between two impenetrable walls obtained by DDD simulation (circles) and the numerical solution of the phase field model proposed (full line). Relevant simulation parameters are: $u_0 = 0.26$, $\alpha_{sf} = 5.5$, $\alpha_m = 0.02$.

comparison of the prediction of the continuum theory and DDD simulations can be seen in Fig. 2. The results obtained are published in PRL [4].

We could also generalize the continuum theory of dislocations with two types of dislocation densities ρ_+ and ρ_- . It turned out, that a term we have neglected earlier plays an important role in dislocation pattern formation. In this case the evolution equations for the total dislocation density $\rho = \rho_+ + \rho_-$ and the “geometrically necessary” dislocation density $\kappa = \rho_+ - \rho_-$ read as

$$\begin{aligned}\partial_t \rho &= \partial_x \left\{ \kappa M_0 \partial_x \frac{\delta P}{\delta \kappa} + \rho M_0 \partial_x \frac{\delta P}{\delta \rho} \right\}, \\ \partial_t \kappa &= \partial_x \left\{ \rho M \left[\partial_x \frac{\delta P}{\delta \kappa} \right] + \kappa M_0 \partial_x \frac{\delta P}{\delta \rho} \right\}.\end{aligned}$$

where $M[x]$ is again a nontrivial on/off type mobility function, while M_0 is a constant. It is found if $\kappa \ll \rho$ the phase field functional

$$P(\rho, \kappa, \chi) = \int_D \left\{ -\frac{D}{2} (\Delta \chi)^2 + b \chi \partial_y \kappa + A \rho \ln \left(\frac{\rho}{\rho_0} \right) + T \frac{\kappa^2}{\rho} \right\} dx dy,$$

where A and T are constants, gives the same evolution equations obtained by the systematic coarse graining the equation of motion of individual interacting dislocations (see details in [6]). It was found by the stability analysis of the trivial homogeneous solution of the above system of partial differential equations that the continuum theory derived leads to dislocation pattern formation if the external load is large enough. It is interesting to note that the primary source of instability is related to the on/off type mobility function (responsible for the finite flow stress of the dislocation system), but the last two terms in $P(\rho, \kappa, \chi)$ related to dislocation-dislocation correlations are crucial for the observed length scale selection in dislocation patterning. Since the theory proposed is scale free, i.e. the evolution equations do not contain any parameter with length dimension, the length scale of the patterning is inversely proportional to $\sqrt{\rho}$, that is in agreement with the experimental observation.

Understanding patterning is a nearly 60 years old problem of dislocation theory. The continuum theory we have derived is obtained by linking the microscopic and mesoscale descriptions of the collective motion of dislocations. Our theory is the first one that predict patterning on a non-phenomenological manner. The results obtained are published in PRB [6].

Properties of dislocation avalanches studied by DDD simulations

Experimental evidences obtained during the past decade indicate that if the system size is less then about $100\mu\text{m}$ the mechanical response of the system (stress-stain relation) depends on the system size. This phenomenon is commonly called size effect. Moreover, if one goes below of $10\mu\text{m}$ characteristic sizes the stress strain response obtained contains random irregular steps resulted by the avalanche like collective motion of dislocations. So, the mechanical properties at this scale cannot be described on a deterministic manner.

In order to get a deep insight into the statistical nature of the stress-strain relation we have performed many large scale 2 and 3D discrete dislocation dynamics simulations with different system sizes and initial dislocation configurations. During the simulations the external stress was slowly increased. A typical simulation result can be seen in Fig. 3.

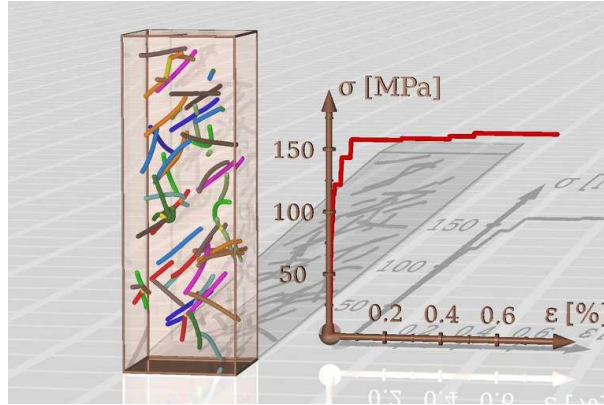


Figure 3: *Typical configuration of 3D DDD simulations together with the stress-strain curve. Dislocation colors denote different glide planes of the fcc crystal structure.*

An important new result obtained is that the regions between avalanches in the individual stress curves as functions of the plastic strain were found nearly linear and reversible (see Fig. 4). In these regions the plastic deformation obeys an effective equation of motion with a nearly linear force. Moreover, for small plastic deformation, the means of the stress-strain curves are power law over two decades. Here and for somewhat larger plastic deformations, the mean stress-strain curves converge for larger sizes, while their variances shrink, both indicating the existence of a thermodynamical limit. In accordance with size-effects from experiments, the converging averages decrease with increasing size. For large plastic deformations, where steady flow sets in, thermodynamical limit was not realized in this model system. At any strain level the probability distribution of stress (corresponding to different realization, i.e. different initial dislocation configuration) follows a Weibull distribution with a Weibull exponent practically independent from the strain level. The results obtained are published in Acta Mat. [2] and PRB [5].

We have also studied in details the properties of strain bursts (dislocation avalanches) occurring in a 2D DDD models under quasistatic stress-controlled loading. Contrary to previous suggestions, the avalanche statistics differs fundamentally from predictions obtained for the depinning of elastic manifolds in quenched random media. Instead, we have found an exponent $\tau = 1$ of the power-law

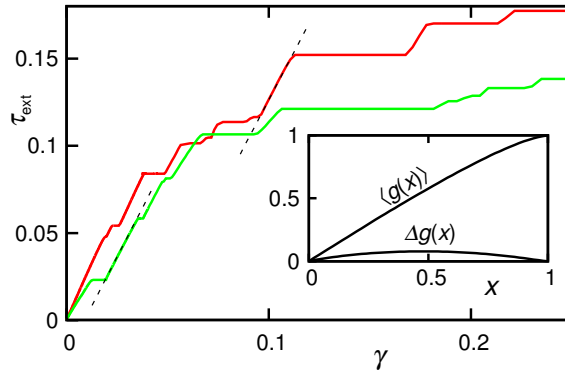


Figure 4: *Stress-strain curves for two realizations obtained by 2D DDD with $N = 512$ dislocations. Segments between plateaus are found to be nearly linear, dashed lines are guide to the eye. Inset: averages of increasing segments normalized to have the same initial and final values. For fixed N 's all fall on the same curve, close to a linear function.*

distribution of slip or released energy, with a cut of that increases exponentially with the applied stress and diverges with system size at all stresses (see Fig. 5).

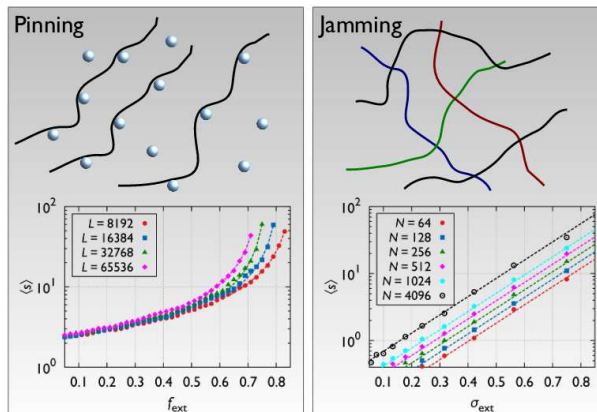


Figure 5: *Differences between pinning and the jamming/unjamming scenario observed for dislocation systems. For pinning/depinning type of transition the mean value of the avalanche size $\langle s \rangle$ is independent from the system size at small external forces, while it diverges at a critical force value. For dislocation systems it always size dependent and no divergence is observed.*

These observations demonstrate that the avalanche dynamics of 2D dislocation systems is scale-free at every applied stress and, therefore, can not be envisaged in terms of critical behavior associated with a depinning transition. The results obtained are published in PRL. [3].

Mesoscopic stochastic model

As it is discussed in the previous section the plastic deformation of crystalline matter often involves intermittent local strain burst events. Similar behavior is also observed for amorphous matter, although in an amorphous structure dislocations cannot exist (the elementary carriers of plasticity are the shear transformation zones). To understand the physical background of the nondeterministic

nature of the stress-strain response observed a minimal stochastic mesoscopic model was introduced, where microstructural details are represented by a fluctuating local yielding threshold. It represents a link between the DDD approach corresponding to the microscale and the fully deterministic continuum descriptions. The model is a cellular automaton (CA) representation of the plastic strain field evolution. The elementary event is the local slip of a cell (achieved in practice by the motion of nearby dislocations), that induces a long-range internal stress redistribution, that may trigger further events. To account for microstructural rearrangements taking place during plastic slip, the local yield threshold is updated on a stochastic manner after each event. The resulting model recovers the stochastic nature of plasticity and yields a power-law distribution for the random steps appearing on the stress-strain curves.

The free parameters of the model are the distribution of the local yield stress and the magnitude (or distribution) of a local slip event. These parameters are representing the microstructural features of the actual material. They have to be determined from a lower level model. In order to do so we performed large scale DDD simulations. We found that the stress value corresponding to the first avalanche follows a Weibull distribution, and the mean stress at the i th avalanche represent a weakest link sequence from the same distribution. This implies that plastic events are local and the subsequent avalanches are weakly correlated confirming the main assumption of the stochastic mesoscopic model. Moreover, with the appropriate choice of the parameters of the Weibull distribution used to get the flow stress values at the updating of the system, the stochastic mesoscopic model is able to reproduce the stress-strain response obtained by DDD. The results obtained are published in two papers [7] and [10].

Micropillar compression tests

In order to experimentally study the plastic deformation properties of micron sized specimens we performed compression tests on micron sized pillars (called micropillar) fabricated into the surface of different (Cu, Zn, Al alloy) single crystals (for details see below). To be able to carry out the compressions we first had to build a micro-compression device suitable to put into the chamber of our SEM (a FEI Quanta 3D). Although, similar devices available commercially, each of them has digital feedback controlling system, resulting a relatively strong integration of the signal measured. So, they are not really suitable to measure the fast avalanches happening during the compression test. To overcome this limitation we have developed a device with fast analogous feedback system.

The sketch and a picture of the device are shown in Fig. 6. Two linear ultrasonic motors are used for the X and Y positioning of the sample. They can move in $0.3\mu m$ steps, but with $10nm$ precision. To be able to detect acoustic emission signal generated during the dislocation avalanches an AE transducer is mounted on the top of the two stages. In Z direction two stages are used. One is a linear step-motor stage used for the “raw” motion of the compressing tip to get it close to the sample. The other one mounted on the linear step-motor stage is a piezoelectric positioning (PEP) stage with about 0.1 nm resolution. During the actual compression test only this stage is moved. To measure the external force a standard spring mounted on the PEP stage is used with strong transverse but very weak longitudinal stiffness. The elongation E of the spring is measured by a capacitive sensor with 0.1 nm resolution. If the PEP stage is moved by the distance P , and the capacitive sensor measures E elongation than the sample deformation is $D = P - E$ and the acting force is $F = SE$, where S is the stiffness of the spring. The pillar compression is performed using a flat punch diamond tip. It should be mentioned that to avoid the charging of the compressing head in the SEM a tip doped by boron has to be used.

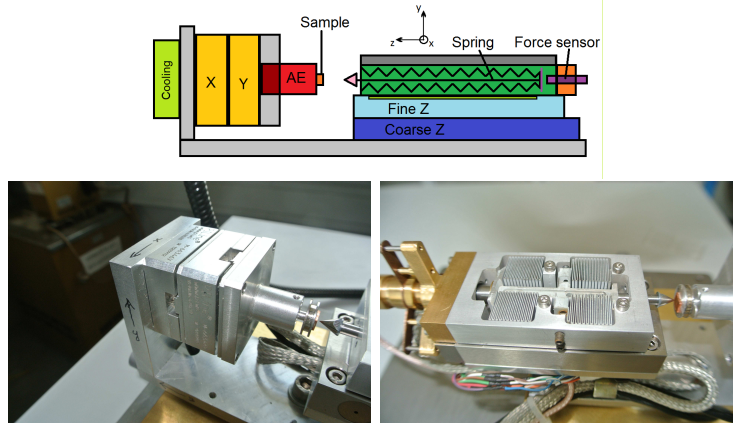


Figure 6: *The sketch and pictures of the micro-compression device.*

Since the statistical analysis of the deformation process of micropillars requires a large number of independent tests we had to develop a new efficient method to fabricate the pillars. They are produced by FIB “digging” a hole around the pillar into the surface of the single crystal. The steps of the fabrication process are described in details in [8].

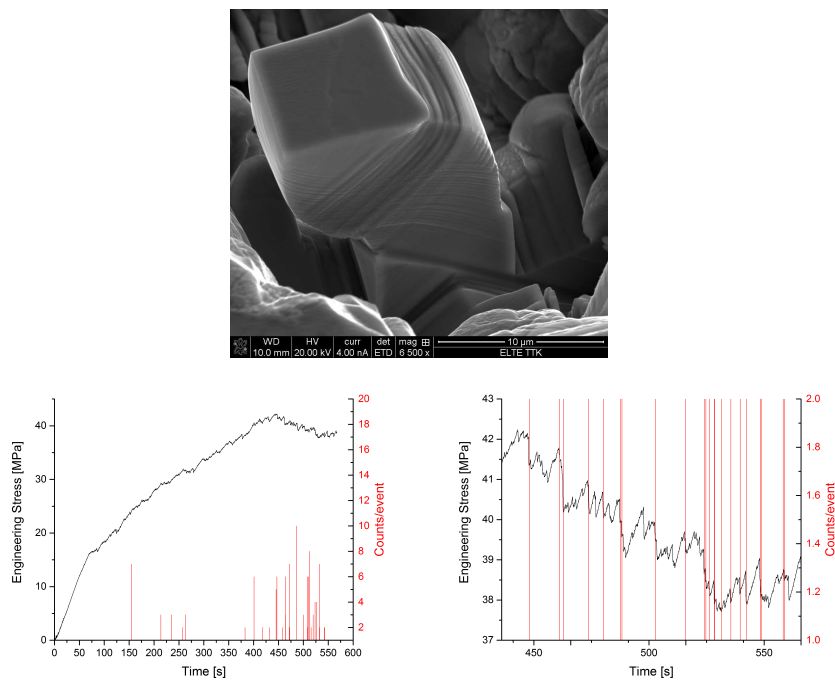


Figure 7: *Compressed micropillar with the corresponding stress versus time curve together with the acoustic emission signal. The right box shows an enlarged part of the curve plotted in the left box. The coincidence between the stress drops and the acoustic emission signals can be seen.*

Typical results obtained can be seen in Fig. 7. (For a movie of an in situ compression see <http://metal.elte.hu/~groma/micropillar/compression.mp4>) It is important to note that with the device developed we found much more small stress drops than in the earlier investigations presented in the literature. This is due to the fast analogous feedback introduced and the enhanced sensitivity

of the force measurement. Moreover, for the first time we could detect directly acoustic emission signal generated during the compression of a micropillar.

X ray line profile and internal stress distribution measurements

Based on the cross correlation analysis of the Kikuchi diffraction patterns high-resolution EBSD (HR-EBSD) is a well established method to determine the internal stress in deformed crystalline materials. In many cases, however, the stress values obtained at the different scanning points have a large (in the order of GPa) scatter. As it was first demonstrated by Wilkinson and co-workers this is due to the long tail of the probability distribution of the internal stress ($P(\sigma)$) generated by the dislocations present in the system. According to the theoretical investigations of the PI and co-workers the tail of $P(\sigma)$ is inverse cubic with prefactor proportional to the total dislocation density $\langle \rho \rangle$. This opens a new possibility to determine important microstructural parameters by EBSD but there are several open issues need to be resolved before the method can be used in a routine way.

To address some of the issues, HR-EBSD results obtained on compressed Cu single crystals were compared to X-ray diffraction (XRD) line profile analysis, that is a well established experimental technique for determining microstructural parameters such as coherent domain size, dislocation density, its fluctuation, and polarization of the dislocation system. As shown by the earlier work of the PI in the so-called "strain broadening" setup the three leading terms at the tail of the intensity distribution $I(q)$ read as

$$I(q) = \frac{1}{\pi^2 d} \frac{1}{q^2} + \frac{\Lambda}{4\pi^2} \langle \rho \rangle \frac{1}{q^3} + \frac{3}{8\pi^3} \langle s \rangle \frac{q}{|q^5|} \quad |q| > q_0$$

where $q = 2[\sin(\Theta) - \sin(\Theta_0)]/\lambda$, d is the coherent domain size, $\langle \rho \rangle$ is the average dislocation density, $\langle s \rangle$ is a parameter proportional to the net polarization of the dislocation system, and λ is the wavelength of the X-rays. Θ and Θ_0 are the half of the scattering angle and the Bragg angle, respectively. The parameter Λ is commonly given in the form $\Lambda = 2|\vec{g}|^2|\vec{b}|^2C_g/\pi$ where \vec{b} and \vec{g} are the Burgers and the diffraction vector, respectively. C_g is called the *diffraction contrast factor* and depends on the type of the dislocation and the relative geometrical position between the dislocation line direction and the direction of \vec{g} . Considering that the tail of the experimental intensity curve can be rather noisy the actual values of the domain size and the dislocation density can be better obtained from the integral quantity

$$M_2(q) = \int_{-q}^q q'^2 I(q') dq'$$

called as second order restricted moment. In the large q regime it reads as

$$M_2(q) = \frac{1}{\pi^2 d} q + \frac{\Lambda}{2\pi^2} \langle \rho \rangle \ln\left(\frac{q}{q_0}\right)$$

where q_0 is a constant depending on the dislocation-dislocation correlation. If the coherent domain size is larger than of about $1 \mu\text{m}$ the first term becomes negligible beside the contribution of dislocations and the plot of M_2 versus $\ln(q)$ becomes a straight line in the asymptotic regime $q \rightarrow \infty$. Its slope is proportional to the mean dislocation density. Using this feature the dislocation density can be determined with an accuracy of a few percent. Since the tail of the internal stress distribution is also inverse cubic the second order restricted moment calculated from the stress distribution is also linear in $\ln(\sigma)$ with slope again proportional to the dislocation density.

Since the software required for HR-EBSD internal stress analysis is not commercially available, as a first step, we had to develop our own software. After this HR-EBSD analysis were performed

on Cu single crystals deformed up to 6 and 10%. X-ray profiles were also determined on the same samples.

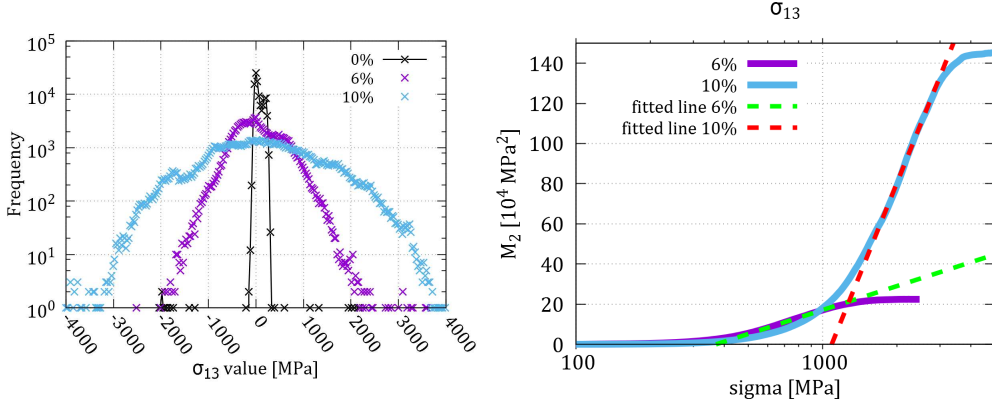


Figure 8: *The probability distribution of the σ_{13} stress component at strains of 0%, 6% and 10% , and the corresponding M_2 versus $\ln(\sigma)$ for the deformed samples, with the straight lines fitted in the asymptotic regime.*

It is found that the dislocation density $\langle \rho \rangle$ determined from $P(\sigma)$ is about the same obtained from X-ray line profile (for details see [9]). This opens further perspectives for the application of EBSD in determining mesoscale parameters in a heterogeneous sample.

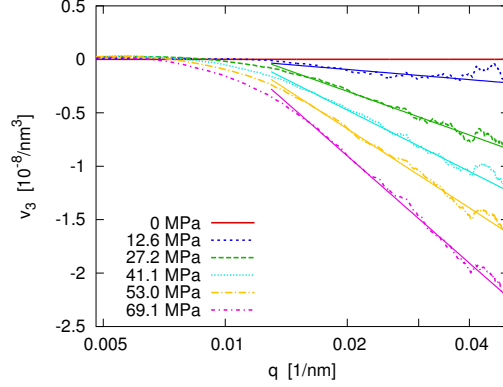


Figure 9: *The $M_3(q)$ restricted moments at different external stress levels which are below the flow stress. For easier interpretation the $M_3(q)$ curve obtained on the unloaded sample is subtracted from the curves.*

Another issue studied during the project is related to the fact that an external load, even if smaller than the flow stress, generates dislocation rearrangement leading to a net polarization of the system. According to the theory of X-ray line broadening explained above, this polarization leads to Bragg peak asymmetry. We have found a direct experimental validation of the theory by in situ profile measurements on an “elastically” deformed Cu single crystals. The profiles are evaluated by the third order restricted moments defined as

$$M_3(q) = \int_{-q}^q q'^3 I(q') dq' \approx \frac{3}{4\pi^3} \langle s \rangle \ln(q/q_1),$$

where q_1 is a constant. In agreement with the theory it is found that peak asymmetry is increasing with deformation (for details see [1]).

List of publications

- [1] I Groma, D Tüzes, PD Ispánovity, Asymmetric X-ray line broadening caused by dislocation polarization induced by external load, *Scripta Materialia* 68 (9), 755-758 (2012)
- [2] PD Ispánovity, Á Hegyi, I Groma, G Györgyi, K Ratter, D Weygand, Average yielding and weakest link statistics in micron-scale plasticity, *Acta Materialia* 61 (16), 6234-6245 (2013)
- [3] PD Ispánovity, L Laurson, M Zaiser, I Groma, S Zapperi, MJ Alava, Avalanches in 2D dislocation systems: Plastic yielding is not depinning, *Physical Review Letters* 112 (23), 235501 (2014)
- [4] I Groma, Z Vandrus, PD Ispánovity, Scale-free phase field theory of dislocations *Physical Review Letters* 114 (1), 015503 (2015)
- [5] P Szabó, PD Ispánovity, I Groma, Plastic strain is a mixture of avalanches and quasireversible deformations: Study of various sizes *Physical Review B* 91 (5), 054106 (2015)
- [6] I Groma, M Zaiser, PD Ispánovity, Dislocation patterning in a two-dimensional continuum theory of dislocations *Physical Review B* 93 (21), 214110 (2016)
- [7] PD Ispánovity, D Tüzes, P Szabó, M Zaiser, I Groma, The role of weakest links and system size scaling in multiscale modeling of stochastic plasticity arXiv preprint arXiv:1604.01645, Accepted for publication in *Physical Review B* (2016)
- [8] Á Hegyi, PD Ispánovity, M Knapek, D Tüzes, K Máthis, F Chmelík, Z Dankházi, G Varga, I Groma, Micron-scale deformation: a coupled in-situ study of strain bursts and acoustic emission arXiv preprint arXiv:1604.01815, Submitted for publication to *Microscopy and Microanalysis* (2016)
- [9] S Kalácska, I Groma, A Borbély, PD Ispánovity, Comparison of the dislocation density obtained by HR-EBSD and X-ray profile analysis, arXiv preprint arXiv:1610.08915, Submitted for publication to *Applied Physics Letters* (2016)
- [10] D Tüzes, M Zaiser, PD Ispánovity, Disorder is good for you: The influence of local disorder on strain localization and ductility of strain softening materials, arXiv preprint arXiv:1604.01821, Submitted for publication to *International Journal of Fracture* (2016)